

# Adaptive Mesh Refinement for Thin-Film Equations

Junseok KIM\*

Department of Mathematics, University of Dongguk, Seoul 135-703

(Received 4 August 2006)

An adaptive finite difference method is developed for a class of fully nonlinear time-dependent thin liquid film equations. Equations of the type  $h_t + f_y(h) = -\epsilon^3 \nabla \cdot (M(h) \nabla \Delta h)$  arise in the context of thin liquid films driven by a thermal gradient with a counteracting gravitational force, where  $h = h(x, y, t)$  is the fluid film height. Enhanced accuracy for the method is attained by covering the front with a sequence of nested, progressively finer, rectangular grid patches that dynamically follow the front motion. Results of numerical experiments illustrate the accuracy, the efficiency, and the robustness of the method.

PACS numbers: 07.05.T, 68.15.+e

Keywords: Adaptive mesh refinement, Nonlinear diffusion equations, Thin film, Nonlinear multigrid method

## I. INTRODUCTION

Thin coating flows are of great technical and scientific interest [1]. Practical examples include manufacturing processes, such as the production of videotapes, photographic films, and microchips [2]. Flows created by gradients in surface tension, whether induced by temperature or concentration variations, are commonly called thermocapillary or Marangoni-driven flows. For very thin capillary driven films, an experiment shows that the Marangoni stress causes a capillary ridge to form and the film to finger (see Fig. 1(a)).

Most previous numerical studies of lubrication-type flows have focused on overcoming the stability requirement for explicit schemes that the time step  $\Delta t$  should be  $O(\Delta x^4)$  - a prohibitive restriction. Alternating-direction implicit (ADI) algorithms enable time steps several orders of magnitude larger than  $O(\Delta x^4)$  to be used successfully [3].

The objective of this paper is to describe the extension of our single grid algorithm for the thin film equations [4] to an adaptive mesh refinement algorithm so that we can simulate realistic physical phenomena. This paper is organized as follows. In Section II we briefly review the governing equations. In Section III, we derive the numerical solution with a nonlinear multigrid method. In Section IV, we present numerical results. Conclusions are made in Section V.

## II. GOVERNING EQUATIONS

We consider the dynamics of a thin layer of liquid of thickness  $h$  on an inclined surface driven by thermally

created surface tension gradients and influenced by gravity (see Fig. 1(b)). The spatial variables  $x$  and  $y$  denote the direction normal to the flow and the direction of the flow, respectively. Let  $\alpha$ ,  $\rho$ ,  $g$ ,  $\eta$ ,  $\gamma$ , and  $\tau = d\gamma/dy$  denote the angle from a horizontal inclination of the plane, the density, the gravitational constant, the dynamic viscosity, the surface tension, and the surface tension gradi-

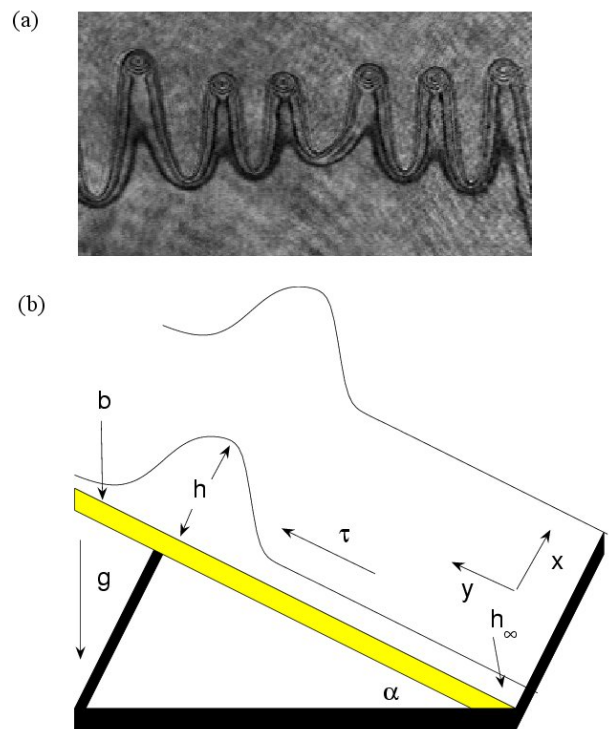


Fig. 1. (a) A thin film flow climbs up an inclined plate, which is driven by Marangoni stresses, against gravity. (b) A schematic diagram of the physical problem.

\*E-mail: cfdkim@dongguk.edu

ent of the liquid, respectively. We model the dynamics of the draining film by using the lubrication approximation with a “depth averaged” velocity [5],

$$\vec{V} = \left( \frac{\tau h}{2\eta} - \frac{\rho g h^2 \sin \alpha}{3\eta} \right) \vec{e}_y + \frac{\gamma h^2 \nabla \Delta h}{3\eta}. \quad (1)$$

The coefficient of  $\vec{e}_y = (0, 1)$  in Eq. (1) represents convection due to the surface tension gradient and the component of gravity tangent to the surface. We couple Eq. (1) with mass conservation,  $h_t + \nabla \cdot (h\vec{V}) = 0$ . We rescale to dimensionless units as in Ref. [5]:  $h = H\hat{h}$ ,  $(x, y) = l(\hat{x}, \hat{y})$ , and  $t = T\hat{t}$ , where  $H = \frac{3\tau}{2\rho g \sin \alpha}$ ,  $l = (\frac{2\gamma H^2}{3\tau})^{1/3}$ , and  $T = (\frac{16\gamma\eta^3}{3\tau^4 H})^{1/3}$ . Dropping the  $\hat{\phantom{x}}$  gives the dimensionless equation

$$h_t + (h^2 - h^3)_y = -\nabla \cdot (h^3 \nabla \Delta h). \quad (2)$$

In the model, we take  $y = 0$  to be the position of the edge of the meniscus. For the boundary condition at  $y = 0$ , we assume the meniscus has just pinched off a film of thickness  $h(x, 0, t) = h_\infty$  with zero third derivative  $h_{yyy}(x, 0, t) = 0$ , *i.e.*, that the meniscus enforces a zero net curvature gradient on the bulk-film region [6]. We choose the simplest boundary condition consistent with complete wetting, that of a precursor model in which  $h \rightarrow b > 0$  as  $y \rightarrow \infty$  [7,8].

We can think of the traveling wave as a viscous regularization of a shock wave if we rescale the space and the time variables by  $(x', y') = \epsilon(x, y)$  and  $t' = \epsilon t$ ; then, Eq. (2) becomes, after dropping the  $'$  notation,

$$h_t + (h^2 - h^3)_y = -\epsilon^3 \nabla \cdot (h^3 \nabla \Delta h). \quad (3)$$

This equation is a fourth order nonlinear singular perturbation of the conservative law  $h_t + (h^2 - h^3)_y = 0$ , which has a nonconvex flux function  $f(h) = h^2 - h^3$  [9].

### III. NUMERICAL METHOD

We split Eq. (3) into a system of the following form:

$$h_t + f_y(h) = \nabla \cdot (M(h)\nabla\mu), \quad (4)$$

$$\mu = -\epsilon^3 \Delta h, \quad (5)$$

where  $M(h) = h^3$ . Let  $h_{ij}^n$  be an approximation of  $h(x_i, y_j, t_n)$ , where  $x_i = (i - 0.5)\Delta x$ ,  $y_j = (j - 0.5)\Delta x$ , and  $t_n = n\Delta t$ . Now, we present a semi-implicit time and centered difference space discretization of Eqs. (4) and (5):

$$\frac{h_{ij}^{n+1} - h_{ij}^n}{\Delta t} = \nabla_d \cdot \left[ \frac{M(h)_{ij}^{n+1}}{2} \nabla_d \mu_{ij}^{n+1} \right] + \nabla_d \cdot \left[ \frac{M(h)_{ij}^n}{2} \nabla_d \mu_{ij}^n \right] - f_y(h_{ij}^n). \quad (6)$$

$$\mu_{ij}^{n+1} = -\epsilon^3 \Delta_d h_{ij}^{n+1}. \quad (7)$$

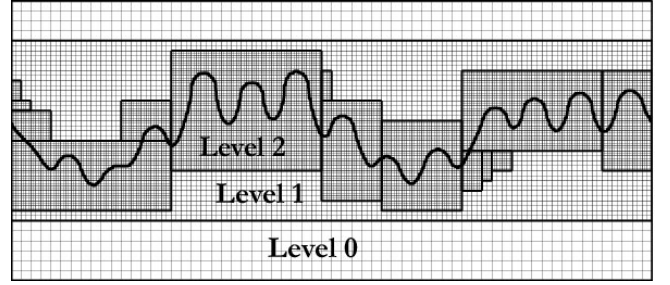


Fig. 2. Block-structured local refinement. In this example, there are three levels.

$f_y(h_{ij}^n)$  is treated by using a second-order essentially non-oscillatory (ENO) scheme [10], *i.e.*,

$$f_y(h_{ij}^n) = f'(h_{ij}^n) \left( \frac{\bar{h}_{i,j+\frac{1}{2}}^n - \bar{h}_{i,j-\frac{1}{2}}^n}{\Delta x} \right).$$

The edge values  $\bar{h}_{i,j+\frac{1}{2}}^n$  are computed as follows:

$$k = \begin{cases} j & f'(h_{i,j+\frac{1}{2}}^n) \geq 0 \\ j+1 & \text{otherwise} \end{cases}$$

$$a = \frac{h_{ik}^n - h_{i,k-1}^n}{\Delta x}, \quad b = \frac{h_{i,k+1}^n - h_{ik}^n}{\Delta x},$$

$$d = \begin{cases} a & \text{if } |a| \leq |b| \\ b & \text{otherwise} \end{cases}$$

$$\bar{h}_{i,j+\frac{1}{2}}^n = h_{ik}^n + \frac{\Delta x}{2} d(1 - 2(k - j)).$$

#### 1. Dynamic Adaptive Mesh Refinement

In Fig. 2, we show an example of the grid structure used in the adaptive mesh refinement (AMR) [11]. In the non-adaptive multigrid on uniform grids, we have used a hierarchy of global grids,  $\Omega_0, \Omega_1, \dots, \Omega_l$ . In the adaptive approach, we introduce a hierarchy of increasingly finer grids,  $\Omega_{l+1}, \dots, \Omega_{l+l^*}$ , restricted to smaller and smaller subdomains. That is, we consider a hierarchy of grids,  $\Omega_0, \Omega_1, \dots, \Omega_{l+0}, \Omega_{l+1}, \dots, \Omega_{l+l^*}$ . We denote  $\Omega_{l+0}$  as level zero,  $\Omega_{l+1}$  as level one, and so on. In Fig. 2 we have  $l^* = 2$ .

The grid is adapted dynamically based on the undivided gradient. First, we tag cells that contain the front, *i.e.*, those in which the undivided gradient of the film height is greater than a critical value. Then, the tagged cells are grouped into rectangular patches by using a clustering algorithm as in Ref. [12]. These rectangular patches are refined to form the grids at the next level. The process is repeated until a specified maximum level is reached.

## 2. Numerical solution - An Adaptive Nonlinear Multigrid Method

In this section, we develop a nonlinear full approximation storage (FAS) multigrid method to solve the nonlinear discrete system, Eqs. (6) and (7), at an implicit time level. See the Ref. [13] for additional details and background. The algorithm of the nonlinear multigrid method for solving the discrete system is as follows:

First, let us rewrite Eqs. (6) and (7) as

$$N(h^{n+1}, \mu^{n+1}) = (\phi^n, \psi^n),$$

where

$$N(h^{n+1}, \mu^{n+1}) = \left( \frac{h_{ij}^{n+1}}{\Delta t} - \nabla_d \cdot \left[ \frac{M(h)_{ij}^{n+1}}{2} \nabla_d \mu_{ij}^{n+1} \right], \right. \\ \left. \mu_{ij}^{n+1} + \epsilon^3 \Delta_d h_{ij}^{n+1} \right)$$

and the source term is

$$(\phi^n, \psi^n) = \left( \frac{h_{ij}^n}{\Delta t} + \nabla_d \cdot \left[ \frac{M(h)_{ij}^n}{2} \nabla_d \mu_{ij}^n \right] \right.$$

$$\left. - f_y(h_{ij}^n), 0 \right).$$

Using the above notations on all levels  $k = 0, 1, \dots, l, l+1, \dots, l+l^*$ , an adaptive multigrid cycle is formally written as follows [13]:

### Adaptive cycle

First we calculate  $\phi_k^n, \psi_k^n$  on all levels and set the previous time solution as the initial guess, *i.e.*,  $(h_k^0, \mu_k^0) = (h_k^n, \mu_k^n)$ .

$$(h_k^{m+1}, \mu_k^{m+1}) = \text{ADAPTIVEcycle} \\ (k, h_k^m, \mu_k^m, N_k, \phi_k^n, \psi_k^n, \nu).$$

#### 1) Presmoothing

- Compute  $(\bar{h}_k^m, \bar{\mu}_k^m)$  by applying  $\nu$  smoothing steps to  $(h_k^m, \mu_k^m)$  on  $\Omega_k$ .

$$(\bar{h}_k^m, \bar{\mu}_k^m) = \text{SMOOTH}^\nu(h_k^m, \mu_k^m, N_k, \phi_k^n, \psi_k^n),$$

where one *SMOOTH* relaxation operator step consists of solving Eqs. (10) and (11) given below by  $2 \times 2$  matrix inversion for each  $i$  and  $j$ . Rewriting Eqs. (6) and (7), we get

$$\frac{h_{ij}^{n+1}}{\Delta t} + \frac{M_{i+\frac{1}{2},j}^{n+1} + M_{i-\frac{1}{2},j}^{n+1} + M_{i,j+\frac{1}{2}}^{n+1} + M_{i,j-\frac{1}{2}}^{n+1}}{2\Delta x^2} \mu_{ij}^{n+1} = \phi_{ij}^n \quad (8)$$

$$+ \frac{M_{i+\frac{1}{2},j}^{n+1} \mu_{i+1,j}^{n+1} + M_{i-\frac{1}{2},j}^{n+1} \mu_{i-1,j}^{n+1} + M_{i,j+\frac{1}{2}}^{n+1} \mu_{i,j+1}^{n+1} + M_{i,j-\frac{1}{2}}^{n+1} \mu_{i,j-1}^{n+1}}{2\Delta x^2}, \\ - \frac{4\epsilon^3}{\Delta x^2} h_{ij}^{n+1} + \mu_{ij}^{n+1} = \psi_{ij}^n - \frac{\epsilon^3}{\Delta x^2} (h_{i+1,j}^{n+1} + h_{i-1,j}^{n+1} + h_{i,j+1}^{n+1} + h_{i,j-1}^{n+1}). \quad (9)$$

Next, we replace  $h_{kl}^{n+1}$  and  $\mu_{kl}^{n+1}$  in Eqs. (8) and (9) with  $\bar{h}_{kl}^m$  and  $\bar{\mu}_{kl}^m$  if  $k \leq i$  and  $l \leq j$ ; otherwise we replace them with  $h_{kl}^m$  and  $\mu_{kl}^m$ , *i.e.*,

$$\frac{\bar{h}_{ij}^m}{\Delta t} + \frac{M_{i+\frac{1}{2},j}^m + M_{i-\frac{1}{2},j}^m + M_{i,j+\frac{1}{2}}^m + M_{i,j-\frac{1}{2}}^m}{\Delta x^2} \bar{\mu}_{ij}^m = \phi_{ij}^n \quad (10)$$

$$+ \frac{M_{i+\frac{1}{2},j}^m \mu_{i+1,j}^m + M_{i-\frac{1}{2},j}^m \mu_{i-1,j}^m + M_{i,j+\frac{1}{2}}^m \mu_{i,j+1}^m + M_{i,j-\frac{1}{2}}^m \mu_{i,j-1}^m}{\Delta x^2}, \\ - \frac{4\epsilon^3 \bar{h}_{ij}^m}{\Delta x^2} + \bar{\mu}_{ij}^m = \psi_{ij}^n - \frac{\epsilon^3 (h_{i+1,j}^m + \bar{h}_{i-1,j}^m + h_{i,j+1}^m + \bar{h}_{i,j-1}^m)}{\Delta x^2}, \quad (11)$$

where  $M_{i+\frac{1}{2},j}^m = M((h_{ij}^m + h_{i+1,j}^m)/2)$  and the other terms are similarly defined.

#### 2) Coarse-grid correction

- Compute

$$(\bar{h}_{k-1}^m, \bar{\mu}_{k-1}^m) = \begin{cases} I_k^{k-1}(\bar{h}_k^m, \bar{\mu}_k^m) & \text{on } \Omega_{k-1} \cap \Omega_k \\ (h_{k-1}^m, \mu_{k-1}^m) & \text{on } \Omega_{k-1} - \Omega_k. \end{cases}$$

- Compute the right-hand side

$$(\phi_{k-1}^n, \psi_{k-1}^n) = \begin{cases} I_k^{k-1} \{ (\phi_k^n, \psi_k^n) - N_k(\bar{h}_k^m, \bar{\mu}_k^m) \} \\ + N_{k-1} I_k^{k-1}(\bar{h}_k^m, \bar{\mu}_k^m) & \text{on } \Omega_{k-1} \cap \Omega_k \\ (\phi_{k-1}^n, \psi_{k-1}^n) & \text{on } \Omega_{k-1} - \Omega_k. \end{cases}$$

- Compute an approximate solution  $(\hat{h}_{k-1}^m, \hat{\mu}_{k-1}^m)$  of the coarse grid equation on  $\Omega_{k-1}$ , *i.e.*,

$$N_{k-1}(h_{k-1}^m, \mu_{k-1}^m) = (\phi_{k-1}^n, \psi_{k-1}^n). \quad (12)$$

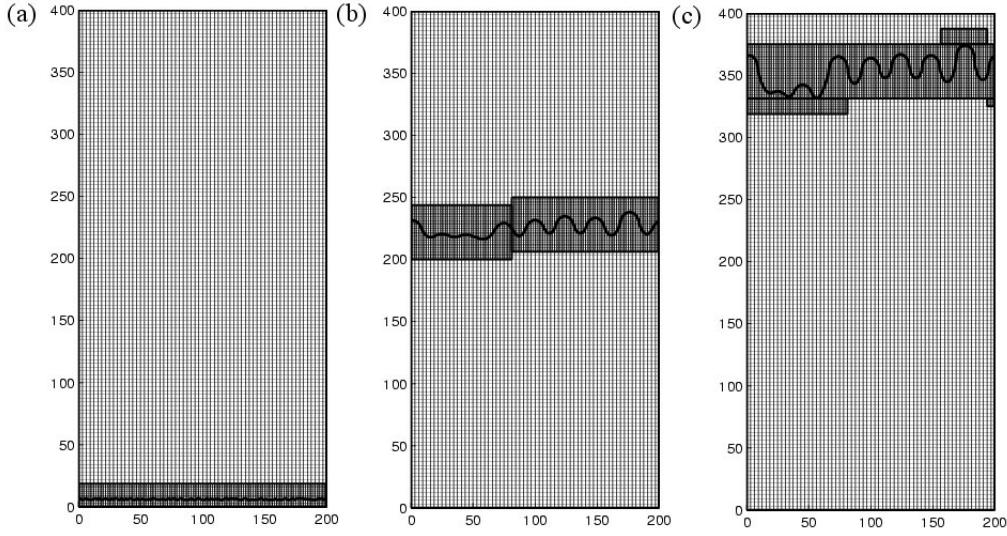


Fig. 3. Evolution of the fluid front is shown from left to right. The times are  $t = 0, 1875,$  and  $2850$ . There are two levels, and the effective fine mesh is  $128 \times 256$ .

If  $k = 1$ , we explicitly invert a  $2 \times 2$  matrix to obtain the solution. If  $k > 1$ , we solve Eq. (12) by using  $(\bar{h}_{k-1}^m, \bar{\mu}_{k-1}^m)$  as an initial approximation to perform an adaptive multigrid  $k$ -grid cycle:

$$(\hat{h}_{k-1}^m, \hat{\mu}_{k-1}^m) = \text{ADAPTIVEcycle}(k-1, \bar{h}_{k-1}^m, h_{k-2}^m, \bar{\mu}_{k-1}^m, \mu_{k-2}^m, N_{k-1}, \phi_{k-1}^n, \psi_{k-1}^n, \nu).$$

- Compute the correction at  $\Omega_{k-1} \cap \Omega_k$ .

$$(\hat{u}_{k-1}^m, \hat{v}_{k-1}^m) = (\hat{h}_{k-1}^m, \hat{\mu}_{k-1}^m) - (\bar{h}_{k-1}^m, \bar{\mu}_{k-1}^m).$$

- Set the solution at the other points of  $\Omega_{k-1} - \Omega_k$ .

$$(h_{k-1}^{m+1}, \mu_{k-1}^{m+1}) = (\hat{h}_{k-1}^m, \hat{\mu}_{k-1}^m).$$

- Interpolate the correction to  $\Omega_k$ ,  $(\hat{u}_k^m, \hat{v}_k^m) = I_{k-1}^k(\hat{u}_{k-1}^m, \hat{v}_{k-1}^m)$ .

- Compute the corrected approximation on  $\Omega_k$ .

$$(h_k^m, \mu_k^m) = (\bar{h}_k^m + \hat{u}_k^m, \bar{\mu}_k^m + \hat{v}_k^m).$$

### 3) Postsmoothing

$$(h_k^{m+1}, \mu_k^{m+1}) = \text{SMOOTH}^\nu$$

$$(h_k^m, \mu_k^m) = (\bar{h}_k^m, \bar{\mu}_k^m, N_k, \phi_k^n, \psi_k^n).$$

This completes the description of a nonlinear ADAPTIVE cycle.

## IV. NUMERICAL RESULTS

In this section, we validate our scheme by comparison with previously reported numerical results. We then present an example to show the power of the adaptive mesh refinement method in computing the evolution of a thin liquid film. We are concerned here with the slow flow

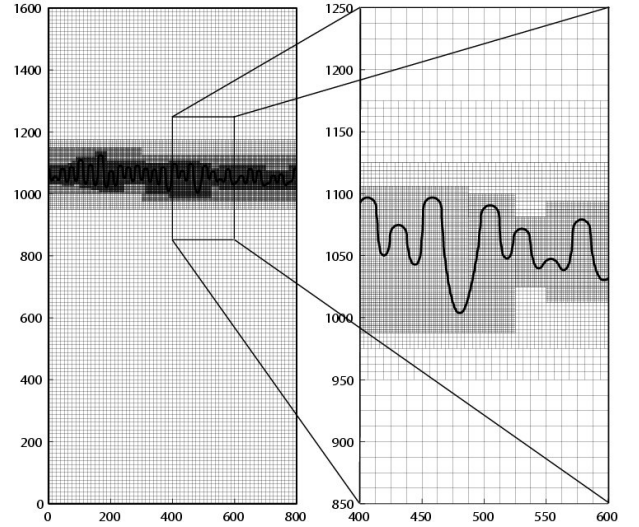


Fig. 4. (Left) There are four levels, and the effective fine grid resolution is  $1024 \times 2048$ . This figure displays the fingering phenomenon at  $t = 7800$ . (Right) A close-up view of the mesh refinement around the front.

of a thin liquid layer on a solid or a substrate. Slight perturbations of the base state, applied along the front, initiate the fingering instability. The mathematical model (Eq. (3)) will be used for a numerical simulation of fingering flows. The initial condition is

$$h(x, y, 0) = 0.5[h_\infty + b - (h_\infty - b) \tanh(3(y - 7) + \text{rand}(x, y))],$$

where  $h_\infty = 0.2$ ,  $b = 0.002$ , and  $\text{rand}(x, y)$  is a random number in  $[-1, 1]$ . These perturbations model deviations from the straight front in the experiments. The computational domain using an effective fine resolution of

$128 \times 256$  is  $\Omega = [0, 200] \times [0, 400]$ . The uniform time step  $\Delta t = 1.0$  and  $\epsilon^3 = 100$  are used. Fig. 3 shows the evolution of the fluid front at  $t = 0$ , 1875, and 2850.

The main result of the present study is shown in Fig. 4 (left), which directly establishes the efficiency of our method. In Fig. 4 (right), a close-up view of the adaptive mesh refinement around the front is illustrated. The effective fine resolution is  $1024 \times 2048$ . Compared with the elapsed time, the new adaptive method is more than 1000 times faster than the preceding uniform mesh method [4].

## V. CONCLUSION

In this paper, we described an adaptive mesh refinement algorithm for thin liquid film equations. In our adaptive mesh refinement computations, we observed many orders of adaptive speed-up compared to uniform mesh computations. As a future research plan, this powerful adaptive mesh refinement algorithm will be applied to the simulation of quantum dot being formed by a molecular beam [14–18] as we did in Refs. [19–21] for uniform meshes.

## ACKNOWLEDGMENTS

This work is supported by the Dongguk University Research Fund.

## REFERENCES

- [1] T. G. Myers, *SIAM Rev.* **40**, 441 (1998).
- [2] C. H. Ho and Y. C. Tai, *Annu. Rev. Fluid Mech.* **30**, 579 (1998).
- [3] D. E. Weidner, L. W. Schwartz and M. H. Eres, *J. Colloid Interface Sci.* **187**, 243 (1997).
- [4] J. S. Kim and J. Sur, *Commun. Korean Math. Soc.* **20**, 179 (2005).
- [5] A. L. Bertozzi, A. Münch, X. Fanton and A. M. Cazabat, *Phys. Rev. Lett.* **81**, 5169 (1998).
- [6] J. Sur, A. L. Bertozzi and R. P. Behringer, *Phys. Rev. Lett.* **90**, 126105 (2003).
- [7] A. L. Bertozzi and M. P. Brenner, *Phys. Fluids* **9**, 530 (1997).
- [8] S. M. Troian, E. Herbolzheimer, S. A. Safran and J. F. Joanny, *Europhys. Lett.* **10**, 25 (1989).
- [9] A. L. Bertozzi, A. Münch and M. Shearer, *Physica D* **134**, 431 (1999).
- [10] C. W. Shu and S. Osher, *J. Comp. Phys.* **83**, 32 (1989).
- [11] A. S. Almgren, J. B. Bell, P. Colella, L. H. Howell and M. L. Welcome, *J. Comp. Phys.* **142**, 1 (1998).
- [12] M. J. Berger and I. Rigoustos, Technical Report NYU-501, New York University-CIMS, 1991.
- [13] U. Trottenberg, C. Oosterlee and A. Schuller, *MULTI-GRID* (Academic Press, U.S.A., 2001), p. 372.
- [14] S. J. Park, H. T. Lee, J. H. Kim and T. Y. Seong, *J. Korean Phys. Soc.* **31**, 537 (1997).
- [15] Y. M. Park, Y. J. Park, K. M. Kim, C. H. Roh, C. K. Hyon and E. K. Kim, *J. Korean Phys. Soc.* **37**, 984 (2000).
- [16] J. H. Seok and J. Y. Kim, *J. Korean Phys. Soc.* **39**, S393 (2001).
- [17] M. H. Jung, S. H. Park, K. H. Kim, H. S. Kim, J. H. Chang, D. C. Oh, T. Yao, J. S. Song and H. J. Ko, *J. Korean Phys. Soc.* **49**, 890 (2006).
- [18] J. S. Kim and J. S. Kim, *J. Korean Phys. Soc.* **49**, 195 (2006).
- [19] S. M. Wise, J. S. Kim and W. C. Johnson, *Thin Solid Films* **473**, 151 (2005).
- [20] S. M. Wise, J. S. Lowengrub, J. S. Kim and W. C. Johnson, *Superlatt. Microstruc.* **36**, 293 (2004).
- [21] S. M. Wise, J. S. Lowengrub, J. S. Kim, K. Thornton, P. W. Voorhees and W. C. Johnson, *Appl. Phys. Lett.* **87**, 133102-1 (2005).